

# Chromosomal association of Ran during meiotic and mitotic divisions

Beth Hinkle<sup>1,2</sup>, Boris Slepchenko<sup>1</sup>, Melissa M. Rolls<sup>3</sup>, Tobias C. Walther<sup>4</sup>, Pascal A. Stein<sup>3</sup>, Lisa M. Mehlmann<sup>1</sup>, Jan Ellenberg<sup>4</sup> and Mark Terasaki<sup>1,2,\*</sup>

<sup>1</sup>Department of Physiology, University of Connecticut Health Center, Farmington, CT 06032, USA

<sup>2</sup>Marine Biological Laboratory, Woods Hole, MA 02543, USA

<sup>3</sup>Department of Cell Biology and Howard Hughes Medical Institute, Harvard Medical School, Boston, MA 02115, USA

<sup>4</sup>European Molecular Biology Laboratory, Meyerhofstrasse 1, 69117 Heidelberg, Germany

\*Author for correspondence (e-mail: terasaki@neuron.uconn.edu)

Accepted 3 September 2002

Journal of Cell Science 115, 4685-4693 © 2002 The Company of Biologists Ltd

doi:10.1242/jcs.00136

## Summary

Recent studies in *Xenopus* egg extracts indicate that the small G protein Ran has a central role in spindle assembly and nuclear envelope reformation. We determined Ran localization and dynamics in cells during M phase. By immunofluorescence, Ran is accumulated on the chromosomes of meiosis-II-arrested *Xenopus* eggs. In living cells, fluorescently labeled Ran associated with the chromosomes in *Xenopus* and remained associated during anaphase when eggs were artificially activated. Fluorescent Ran associated with chromosomes in mouse eggs, during meiotic maturation and early embryonic divisions in

starfish, and to a lesser degree during mitosis of a cultured mammalian cell line. Chromosomal Ran undergoes constant flux. From photobleach experiments in immature starfish oocytes, chromosomal Ran has a  $k_{off}$  of  $\sim 0.06$  second<sup>-1</sup>, and binding analysis suggests that there is a single major site. The chromosomal interactions may serve to keep Ran-GTP in the vicinity of the chromosomes for spindle assembly and nuclear envelope reformation.

Key words: Cell division, Chromosomes, G-proteins, Meiosis, Mitosis, Nuclear proteins

## Introduction

The function of the small GTPase Ran was first studied in mutants, where its absence led to many defects such as in DNA replication, nuclear envelope structure, chromatin structure and cell cycle progression (reviewed in Sazer, 1996; Moore, 2001). A cell-free system led to the recognition of the importance of Ran in nuclear transport, and Ran now has a well established, central role in that process (e.g. Mattaj and Englmeier, 1998; Gorlich and Kutay, 1999). Recently, work with another cell-free system has implicated Ran in M phase processes; this work has been extensively reviewed (e.g. Sazer and Dasso, 2000; Kahana and Cleveland, 2001; Dasso, 2001). In retrospect, the multiple functions of Ran in interphase and M phase are consistent with the many defects observed in the first mutant studies.

The M phase studies have made use of the cell-free extract system from *Xenopus* eggs, where addition of sperm chromatin or DNA coated beads induces the formation of a bipolar microtubule spindle centered on the added DNA. The initial experiments indicated that generation of Ran-GTP was necessary for assembly of the spindle (Wilde et al., 1999; Ohba et al., 1999; Kalab et al., 1999; Carazo-Salas et al., 1999). Importins  $\alpha$  and  $\beta$  have been identified as the target of Ran-GTP; it appears that Ran-GTP displaces microtubule polymerization promoters such as TPX2 or NuMA from importin (Gruss et al., 2001; Nachury et al., 2001; Wiese et al., 2001). A Ran-GTP gradient near the chromosomes in *Xenopus* egg extracts has been visualized (Kalab et al., 2002). In addition to the work on spindle assembly, it has also been

shown that Ran has an essential role in nuclear envelope reformation after mitosis (Zhang and Clarke, 2000; Hetzer et al., 2000; Zhang and Clarke, 2001). There remain unresolved issues about Ran's role in M phase; for instance, verification in living cells of the roles for Ran identified in extracts is required, and has begun to be addressed (Bamba et al., 2002), and to what degree Ran is involved in all eucaryotic cell meiosis and mitoses needs to be resolved.

Light microscopic imaging seems likely to be useful for learning more about Ran and its interactions. For many proteins, the amount of fluorescent analogue required for imaging is in excess of the endogenous protein concentration, which may perturb the natural pathways. Because Ran is one of the most abundant proteins in the cell (Bischoff and Ponstingl, 1991), there should be less danger of disrupting the cell in this way. Another advantage is that Ran's biochemical properties have been well characterized. A major factor in this progress is that Ran is soluble and can be readily produced as a functional recombinant protein (unlike all other small GTPases, Ran has no lipid modifications). Lastly, there is only one isoform of Ran, one known exchange factor and only a few GAPs (GTPase-activating proteins) (Macara et al., 2000), all of which make it simpler to try to interpret observations in living cells. To further investigate Ran during M phase, we have observed fluorescent Ran localization and dynamics in several types of living cells.

## Materials and Methods

Methods for handling *Xenopus* eggs were as described elsewhere

(Terasaki et al., 2001). In brief, immature *Xenopus* oocytes were matured in culture by exposure to 1 µg/ml progesterone; the oocytes became arrested at meiosis II metaphase ~3 hours after white spot formation (Gallo et al., 1995). For immunofluorescence, eggs were fixed in -70°C methanol for 1.5 hours, warmed at room temperature for 30 minutes and then hydrated in 2:1 methanol:PBS (20 minutes), 1:2 methanol:PBS (20 minutes), then PBS. Eggs were incubated in 2.5 µg/ml anti-Ran monoclonal antibody (R32620; Transduction Labs; San Diego, CA) for 1.5 hours followed by 1:50 rhodamine goat anti-mouse (ICN; Costa Mesa, CA) for 1 hour. For DNA double-labeling, eggs were incubated in 10 µg/ml Hoechst dye 33342 (Sigma Chemical Co, St. Louis, MO) for 10 minutes. The eggs were imaged with a Zeiss LSM 410 confocal microscope with UV and visible optics. Hoechst-stained chromosomes can be seen easily in living eggs by wide field fluorescence microscopy (Gallo et al., 1995), but with other fluorescent labels where the contrast is not as high, the spindle region of living or fixed eggs is imaged better by confocal microscopy.

For live cell imaging, Rh-Ran was injected into immature oocytes at a final concentration of 1-2 µM. The endogenous concentration in *Xenopus* oocytes has not been determined. In HeLa cells, Ran is 0.36% of total protein (Bischoff and Ponstingl, 1991); if the total protein concentration is 100 mg/ml in cells, this corresponds to 14 µM (Ran MW 25,000). After maturation, the egg was imaged using an MRC 600 confocal microscope (Bio-Rad; Cambridge, MA) with a krypton argon laser, coupled to an upright microscope with a 40× Plan neofluar N.A. 1.3 objective lens (Zeiss; Thornwood, NY). For photobleaching, a macro was written in the BioRad SOM software to control the scan and image acquisition while the neutral density and laser power levels were switched manually. Quantification was done using public domain NIH Image program (available at <http://rsb.info.nih.gov/nih-image/>).

For imaging anaphase of meiosis II, frog eggs were activated by puncturing the egg surface with a microneedle. The eggs were in an open sided chamber made of silicon rubber (Ronsil, thickness 0.03 inches; North American Reiss, Corp, Blackstone, VA). The needle puncture was done on an upright microscope using a 10× objective lens, then the egg was transferred to a dissecting scope, where a #0 thickness cover slip was placed on top of the egg and maneuvered so that the white spot was positioned straight up. The white spot was located under a 40× oil immersion lens on the confocal microscope, and then scanning was begun to image the calcium wave. Sometimes the wave had already passed, and sometimes it failed to be initiated [later experiments suggested that Ins(1,4,5) $P_3$  injection is more reliable]. With the confocal microscope set to continuous scanning, images were collected on an optical memory disk recorder (Panasonic TQ303F, Secaucus, NJ) with a custom-made trigger circuit.

Fully grown, immature mouse oocytes were collected from the ovaries of PMSG-primed NSA (CF-1) mice (Harlan Sprague-Dawley) in a minimal essential medium (MEM), then washed into MEM without dibutyl cAMP to induce maturation. Matured eggs were microinjected as described previously (Mehlmann and Kline, 1994) and were examined within 30 minutes of injection while being maintained at 37°C on the confocal microscope stage. Rh-Ran was injected in a 3% volume injection, with a resulting final concentration of 2.5 µM.

Starfish (*Asterina miniata*) were obtained from Bodega Bay, CA. Methods for obtaining and handling the gametes were described previously (Jaffe et al., 1993). Mercury-loaded pipettes were used for quantitative microinjection; detailed description of this method and equipment used is available at <http://egg.uchc.edu/injection/>. Embryos were kept in an 18°C incubator until imaged.

Mitotic NRK cells in an injection chamber on a heated microscope stage were pressure injected (<10% volume injection) with a 5:1 mix of Alexa 488 Ran (20 mg/ml) and 70 kDa Rh dextran (2 mg/ml). They were imaged with a Zeiss Planapo 1.4 numerical aperture objective lens using a Zeiss 510 confocal microscope.

## Fluorescent Ran proteins

Tetramethylrhodamine or Alexa 488 was conjugated to the single exposed cysteine (C112) of the three cysteine residues of human Ran (Ribbeck et al., 1998). Both Rh-Ran and Alexa 488-Ran (3 µM) stimulated import of NPC-M9 substrate into digitonin-permeabilized cells as much as wild-type Ran. In this assay, many GTPase cycles are required for import to occur, so if either hydrolysis or exchange on RCC1 were impaired, there would be no import. GTP hydrolysis by both fluorescent conjugates was stimulated by RanGAP with identical kinetics to wild-type Ran. The labeling efficiency of both was greater than 92% in comparison with absorption spectra with tetramethylrhodamine or Alexa 488, so this activity cannot be due to the presence of an active unlabeled fraction. We concluded that Rh-Ran and Alexa 488-Ran are as active as the wild-type unlabeled protein.

GFP-Ran was isolated in a visual screen of a cDNA library concatenated with GFP (VLP55) (Rolls et al., 1999). It consists of an N-terminal GFP followed by a 22 amino-acid linker region (GGGLDPRVRSDDGRGDASGRNAA) and the entire coding sequence for human Ran. GFP-Ran was inserted into the pSP64-S expression vector by standard PCR methods resulting in a consensus echinoderm kozak sequence (aattcaaa). RNA was prepared in vitro using the SP6 mMESSAGE mMACHINE kit (Ambion; Austin, TX). Owing to difficulties in producing GFP-Ran for biochemical characterization, its activity was not tested in vitro.

## Modeling

Photobleaching of chromosomal Ran was followed by exponential recovery. This is consistent with a model based on Ran (or a binding unit containing Ran) binding by mass action kinetics to a single type of binding site. Assuming that the endogenous, fluorescent and bleached forms of Ran behave similarly, the concentrations of bound fluorescent Ran, [R\*B] and bound endogenous Ran, [RB] are described by the equations:

$$d[R*B]/dt = k_{on} [R*][B] - k_{off}[R*B] \quad (1.1)$$

$$d[RB]/dt = k_{on} [R][B] - k_{off}[RB] \quad (1.2)$$

with other notations as follows: [B] is the concentration of free binding sites, [R] is the concentration of free endogenous Ran, [R\*] is the concentration of free fluorescent Ran. Photobleaching converts R\*B into RB but otherwise does not change the steady-state concentrations. This means that [B] =  $B_t - [RB] - [R*B]$  is constant in both equations (1.1 and 1.2) ( $B_t$  is the total concentration of binding sites, both bound and free). If diffusion of Ran in the bleached area equilibrates much faster than binding, [R\*] and [R] can be treated as constants in Equations 1.1 and 1.2. This substantially simplifies the situation, and the solution to Eq. 1.1 is given by a single exponential:

$$[R*B]/[R*] = A [1 - \exp(-k_{off} t)] \quad (2)$$

with  $A = [B]/K_d$  where  $K_d = k_{off}/k_{on}$  is the Ran-binding dissociation constant.

The experimentally observed exponential recovery does not necessarily mean that there is only one type of interaction of Ran with chromosomes. For instance, if there is a second interaction with much larger  $k_{off}$ , there would be a fast recovery for this interaction, which would be complete by the time of the first experimental time point. Also, if the number of binding sites is very different, then the less-abundant site will make only a small contribution to the recovery curve.

For the binding experiments, the experimentally determined values are [R\*B]/[R\*] as a function of added [R\*]. The total amount of fluorescent Ran was known from the quantitative injection. At steady state, there is a higher concentration of Ran in the nucleus than in the cytoplasm, so the total nuclear Ran was calculated by taking into account this difference and the relative volumes of cytoplasm and

nucleus. As follows from Equations 1 under steady-state conditions (adding equations 1.1 and 1.2 then substituting for  $[RB]+[R^*B]$  from the  $B_t$  equation):

$$[B]/K=[RB]/[R]=[R^*B]/[R^*]=B_t(K+[R]+[R^*])^{-1}. \quad (3)$$

The last part of Equation 3 can be used for estimating  $K+[R]$  from experiments with different amounts of  $[R^*]$  by multiplying the experimental  $[R^*B]/[R^*]$  by  $[R^*]$ , which puts the right hand side into the form of the Michaelis-Menten equation with parameters  $V_m=B_t$  and  $K_m=K+[R]$ . The analysis is made somewhat more complex because the endogenous Ran concentration is not known and it is not known whether free Ran or complexed Ran is binding to the chromosomes. When  $\alpha$  is equal to the fraction of the total nuclear Ran (either endogenous or fluorescent), which is available for binding, the expression for  $K_m$  is  $(K/\alpha)+[R]$ .

## Results

### Ran is associated with chromosomes in *Xenopus* and mouse eggs

*Xenopus* eggs are arrested in metaphase of meiosis II. The meiotic spindle is near the surface in a  $\sim 20 \mu\text{m}$  diameter pigment-free region in the central region of the pigmented half of the egg. The spindle axis is oriented perpendicular to the cell surface, so that the chromosomes are arranged more or less in a single plane parallel to and about  $20 \mu\text{m}$  from the egg surface. The chromosomes were labeled with Hoechst dye and Ran was localized by immunofluorescence using a mouse monoclonal antibody originally raised against human Ran that specifically recognizes *Xenopus* Ran (Zhang et al., 1999). Ran fluorescence colocalized with the chromosomes (Fig. 1A).

For imaging Ran localization and dynamics in living eggs, we used a rhodamine-labeled Ran (Rh-Ran). The activity of Rh-Ran was tested in GTPase assays in vitro and behaved identically to unmodified Ran (see Materials and Methods). Microinjected Rh-Ran accumulated at the chromosomes (Fig. 1B). A GFP chimera of Ran was isolated in a visual screen of a cDNA library concatenated with GFP [termed VLP55; (Rolls et al., 1999)]. GFP-Ran, expressed by mRNA injection, also accumulated at the chromosomes (data not shown).

Mature mouse oocytes are arrested in metaphase of meiosis II. As in *Xenopus* eggs, microinjected Rh-Ran localized to the mouse egg chromosomes (Fig. 1C) (Verlhac et al., 2000).

The meiosis II metaphase arrest in *Xenopus* eggs was released by raising intracellular calcium. The egg surface was punctured with a microneedle (prick activation); a calcium wave begins at this point and takes several minutes to cross the egg. Rh-Ran was co-injected with calcium green dextran in order to determine exactly when the calcium wave rose in the spindle region. The Rh-Ran labeled chromosomes began anaphase movements between 12-16 minutes after the calcium rose in the spindle region ( $n=3$ ) (Fig. 2). The timing corresponds well with anaphase onset in cell-free extracts stimulated by addition of calcium (Murray, 1991; Desai et al., 1998). Experiments with Rh-tubulin and calcium green dextran gave the same results (data not shown). Rh-Ran remained associated with the chromosomes at approximately the same brightness. In later stages, Rh-Ran gradually became incorporated into the newly forming nuclear envelope (Fig. 2).

### Chromosomal association of Ran in starfish oocytes and embryos

In order to image Ran throughout meiosis and mitosis, we used starfish oocytes and embryos; they are smaller than frog eggs ( $\sim 180 \mu\text{m}$  versus  $\sim 1.3 \text{ mm}$ ), are optically clear, and are easier to maintain on the microscope stage than mouse eggs. Immature starfish oocytes are arrested in late G2 of meiosis I and possess a large nucleus. Microinjected Rh-Ran, as well as GFP-Ran expressed by mRNA injection, became localized to the nuclear envelope as well as globules near the nuclear envelope. During maturation induced by 1-methyladenine, fluorescence at the nuclear envelope disappeared with nuclear envelope breakdown, whereas the fluorescent globules migrated to the animal pole (Fig. 3A). In oocytes co-injected with Rh-tubulin to label the microtubules, the fluorescent Ran became part of the meiotic spindle and separated at the time of polar body formation (Fig. 3B). This corresponds exactly with the known distribution and behavior of chromosomes in starfish oocytes (Shirai et al., 1990; Ookata et al., 1992).

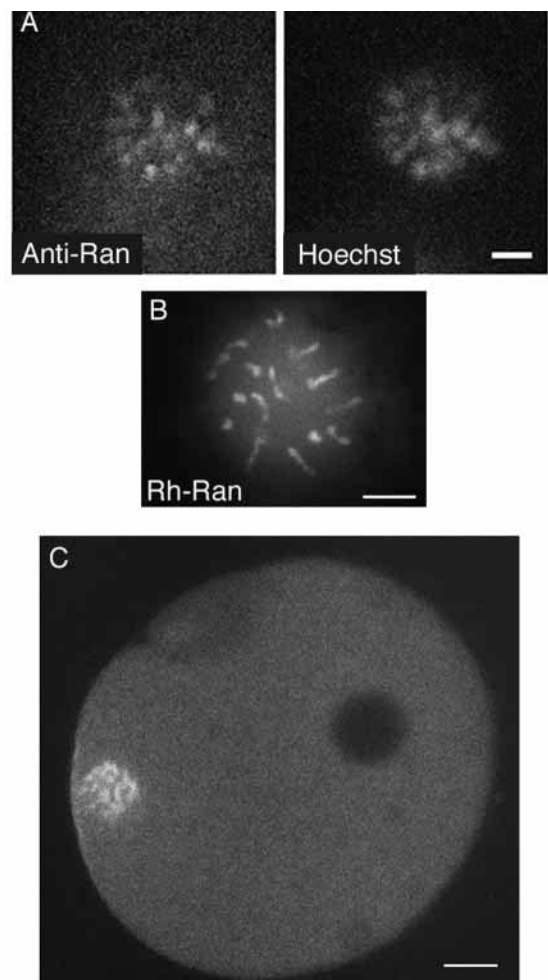


**Fig. 1.** Ran associates with the chromosomes. (A) In meiosis-II-metaphase-arrested *Xenopus* eggs, double-labeling of Ran by immunofluorescence and chromosomes by Hoechst dye shows colocalization of Ran and chromosomes. (B) Microinjected Rh-Ran is associated with the chromosomes in *Xenopus* eggs. (C) Microinjected Rh-Ran is associated with chromosomes in mature mouse eggs. The dark circular region in the egg is the oil drop from the injection. Bars,  $10 \mu\text{m}$ .

Fluorescently labeled Ran was also observed during mitosis in developing embryos. The fluorescent nucleotide Oregon Green dUTP is incorporated into newly synthesized DNA (Carroll et al., 1999) and was used in double labeling experiments in embryonic blastomeres. There was a close correspondence of the Oregon Green dUTP-labeled

chromosomes and Rh-Ran throughout the entire mitotic phase (Fig. 3C). In the mitotic cells as well, microtubules and Ran localized as expected (Fig. 3D).

#### Ran distribution in mitotic mammalian cultured cells

When fluorescent Ran was microinjected into mitotic mammalian cells, it was found to be distributed throughout the mitotic spindle region, with no apparent accumulation on the chromosomes (Fig. 4). However, fluorescent dextran was excluded from the chromosomal regions. When a mixture of 70 kDa Rh-dextran and fluorescent Ran was injected into mitotic NRK (normal rat kidney) cells, the fluorescent dextran was excluded from the region of the chromosomes while the fluorescent Ran was not excluded (Fig. 4). If Ran were not interacting with chromosomes, it should have the same distribution as the dextran. Thus, in mitotic mammalian cultured cells, Ran appears to be associated with chromosomes, although to a lesser degree than in *Xenopus*, mouse or starfish eggs.

#### Quantitative analysis of Ran association with chromosomes

Rh-Ran in a small region of chromosomes was photobleached with intense laser excitation, and the redistribution of the remaining fluorescence was monitored. In meiosis-I-metaphase-arrested *Xenopus* eggs, Rh-Ran fluorescence redistributed to photobleached chromosomal regions with a 50% recovery time of  $11.7 \pm 4.0$  second (s.d.;  $n=8$  eggs) (Fig. 5A,B). In blastula-stage starfish embryos, a bleached area of metaphase-chromosome-associated Rh-Ran recovered to 50% by  $4.7 \pm 1.7$  seconds (s.d.;  $n=5$  cells) (Fig. 5C,D). Owing to the changing shape and position of anaphase chromosomes, we could not determine whether the exchange rates change after the metaphase-anaphase transition.

The chromosomal association of Ran was examined more quantitatively in immature starfish oocytes, where the nucleus is intact but the chromosomes are partially condensed.

The photobleached chromosomal Ran recovery was found to be described very well with an exponential rate constant  $\sim 0.06 \text{ second}^{-1}$ , corresponding to a 50% recovery time of  $\sim 11$  seconds (Fig. 6A). The experimentally observed exponential

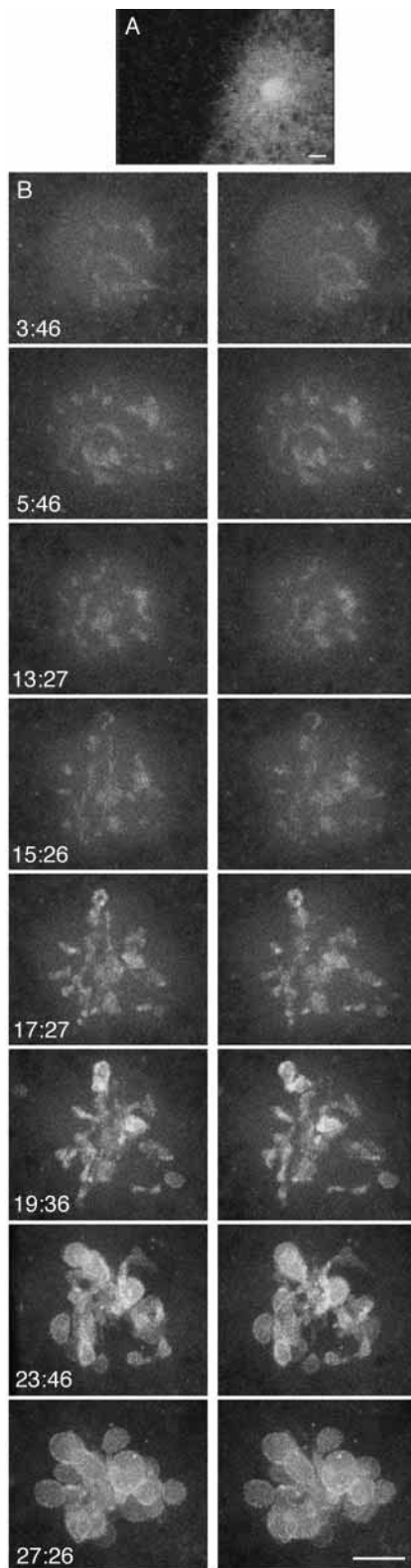


**Fig. 2.** Ran localization in activated *Xenopus* eggs. *Xenopus* oocytes were co-injected with calcium green dextran ( $\sim 15 \mu\text{M}$  final concentration) and Rh-Ran ( $\sim 1.2 \mu\text{M}$ ) then were matured. (A) The matured eggs were prick activated to initiate a calcium wave that releases the meiosis II arrest. The calcium green image shown was taken a few seconds after the calcium wave had passed through the spindle region. The calcium wave is progressing from right to left. The bright circular region is the location of the meiotic spindle; it is bright because of the lack of volume-excluding yolk platelets. (B) Rh-Ran in the meiotic spindle of the egg in the preceding panel was imaged at high magnification. Since the spindle is oriented perpendicularly to the cell surface, it was necessary to take z series sequences to document anaphase movements. z series with a step of  $3.1 \mu\text{m}$  were taken at approximately 2 minute intervals (each series of 14 images took  $\sim 35$  seconds to obtain) and were made into stereo pairs. Timing of the pairs shown is indicated on the figure. Anaphase movements appear to begin between 13 and 15 minutes. Nuclear envelopes reform around individual chromosomes after they have separated (Lemaître et al., 1998); these should later fuse to form a single nucleus but this was not imaged. See stereo movie <http://terasaki.uhc.edu/ran/anaphase.mov>. Bars,  $10 \mu\text{m}$ .

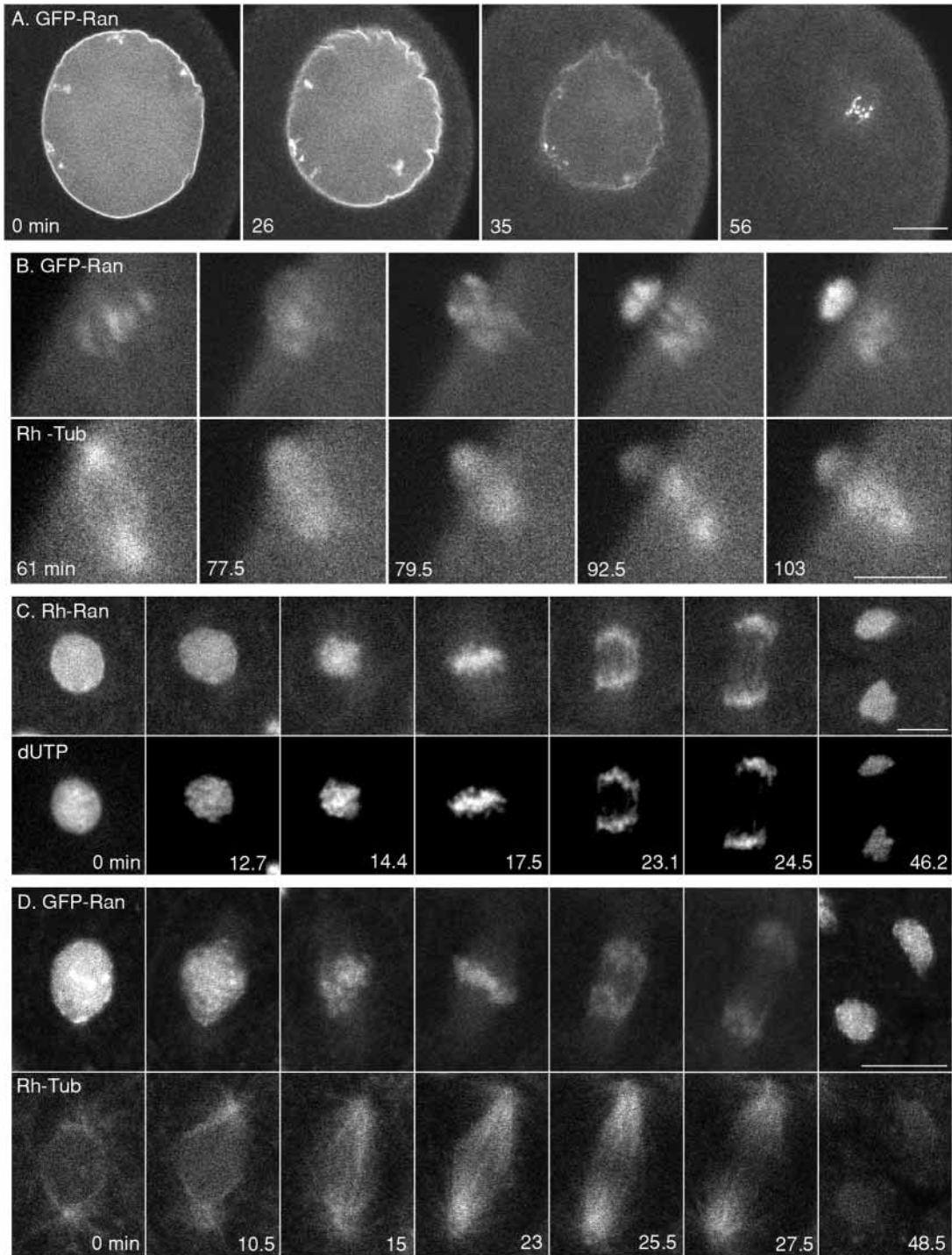


**Fig. 3.** Ran localizes to the chromosomes during meiosis and mitosis in starfish oocytes and embryos. (A) GFP-Ran was expressed in immature starfish oocytes by injection of mRNA. Oocytes were imaged before and during maturation; time elapsed after addition of the maturation hormone 1-methyladenine is indicated. In immature oocytes, GFP-Ran is located at the nuclear envelope. In addition, it is accumulated at globules inside the nuclear envelope. These globules move to the animal pole during maturation. Bar, 25  $\mu\text{m}$ . (B) Double-labeling of Ran and microtubules during meiosis I. GFP-Ran RNA and rhodamine tubulin (5  $\mu\text{M}$  final concentration in cell) were co-injected; after expression of GFP-Ran, the oocyte was matured and imaged. The light/dark border running diagonally is the surface of the oocyte near the animal pole seen from the side, and the sequence shows the extrusion of the first polar body. The location of GFP-Ran with respect to the meiotic spindle is consistent with association with the chromosomes. Bar, 10  $\mu\text{m}$ . (C) Double-labeling of Ran and chromosomes during mitosis. Oocytes were co-injected with Rh-Ran (1.4  $\mu\text{M}$  final concentration in the cell) and Oregon Green 488-5-dUTP (5  $\mu\text{M}$  final concentration in cell), which becomes incorporated into newly synthesized DNA. The oocytes were matured, fertilized and allowed to develop into blastulae, where mitotic divisions were imaged. Rh-Ran appears to colocalize with the DNA label through all stages of mitosis. See movie <http://terasaki.uchc.edu/ran/randutp.mov>. (D) Double-labeling of Ran and microtubules during mitosis. Oocytes were co-injected with GFP-Ran mRNA and rhodamine tubulin as in (B), then matured, fertilized and allowed to develop into blastulae. Bar, 10  $\mu\text{m}$ .

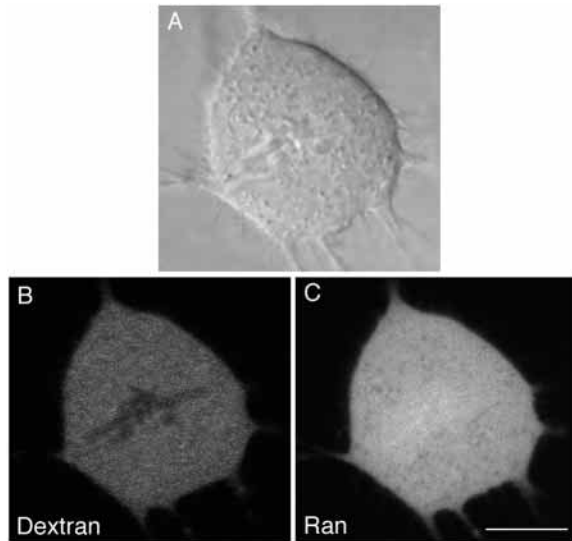
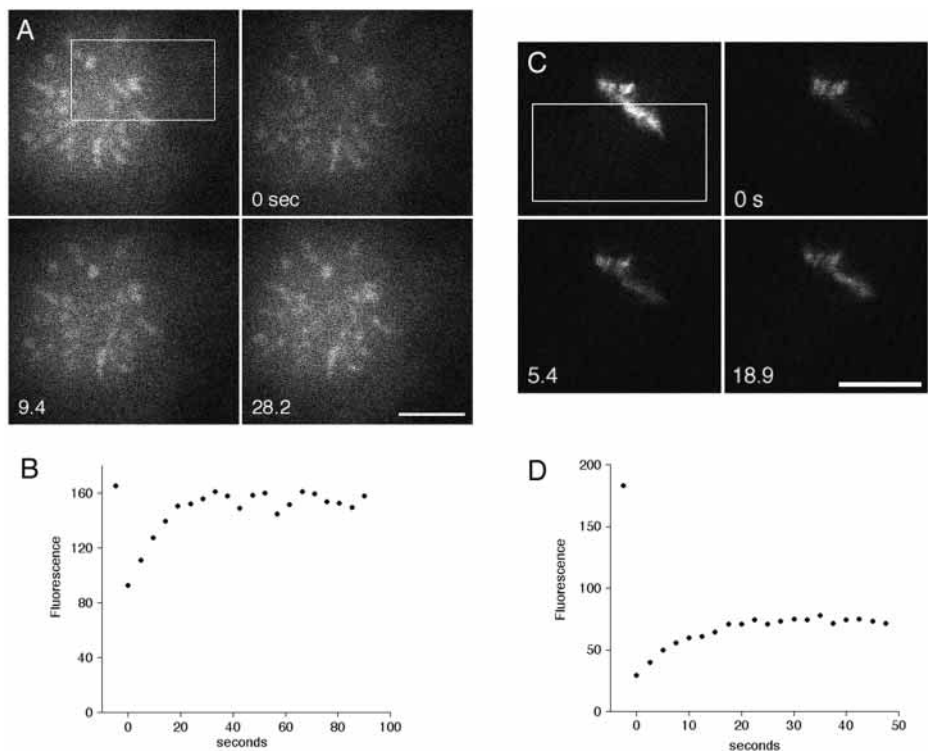


**Fig. 4.** Association of Ran with chromosomes in a cultured mammalian cell. A mitotic NRK cell was injected with Alexa 488 Ran and 70 kDa Rh dextran. (A) The position of the chromosomes is seen in a scanning transmission light image. (B) 70 kDa Rh dextran is excluded from the region of the chromosomes. (C) Fluorescent Ran is present throughout the spindle region, and in particular, in the region of the chromosomes. Since a non-interacting molecule should have a similar distribution to the fluorescent dextran, this is evidence for a Ran association with chromosomes. Bar, 10  $\mu\text{m}$ .

**Fig. 5.** Dynamics of Rh-Ran.

(A) Microinjected Rh-Ran in a *Xenopus* egg was photobleached in the rectangular region shown in the upper left panel, and the recovery was followed in images taken every 4.7 seconds. The photobleach consisted of eight consecutive slow scans lasting 24.8 seconds in the outlined rectangular region, with  $\sim 750\times$  the light intensity as for imaging. As seen in the first post-bleach image, the chromosomes and cytosol became dimmer outside as well as within the bleach zone. This is likely to be a consequence of exchange of cytosolic Rh-Ran with chromosomal Rh-Ran. (B) Time course of fluorescence recovery of one of the chromosomes within the bleached region.

(C) Rh-Ran was microinjected into immature starfish oocytes (final concentration of 1–2  $\mu\text{M}$ ). The oocytes were matured, fertilized and allowed to develop to the blastula stage ( $\sim 128$ –256 cells), where mitotic cells were imaged. Rh-Ran associated with metaphase chromosomes was photobleached in a similar manner as described for *Xenopus* eggs, except the ‘normal’ scan speed of the BioRad confocal microscope was used. The bleach period was eight consecutive scans lasting  $\sim 8.5$  seconds, and images were obtained afterwards every 2.5 seconds; timing of the images shown are indicated on the figure. Bar, 10  $\mu\text{m}$ . (D) Fluorescence recovery of a photobleached region of the metaphase chromosomes. As in *Xenopus*, the parts of the chromosomes that were not irradiated were dimmer immediately after photobleaching. In contrast to *Xenopus* (Fig. 5B), the fluorescence does not return to the original value. The likely explanation is that the bleaching protocol depletes a very small fraction of the total Ran in frog oocytes but depletes a large fraction in the much smaller starfish blastomeres.



recovery is consistent with chromosomal Ran undergoing one major interaction, of the simple type described above, and also allows one to equate the exponential rate constant to the  $k_{\text{off}}$ . Had the experimentally observed recovery been non-exponential, it would not be possible to draw these conclusions.

For simple binding interactions, a standard procedure is to measure the bound ligand as a function of total ligand concentration; this analysis yields the dissociation constant  $K_d$  and the concentration of binding sites. Four different amounts of Rh-Ran were injected into starfish oocytes and allowed to come to equilibrium, then measurements of the brightest part of the chromosome (typically a 1–2  $\mu\text{m}$  diameter region of interest) along with a neighboring nuclear region were made. In oocytes injected with 10 kDa rhodamine dextran and Alexa 488-Ran, the fluorescent dextran was just as bright in the nucleus as in regions of the chromosomal Rh-Ran labeling (Fig. 6B), leading to the conclusion that the soluble Ran can diffuse into the regions of the chromosomes. All of the chromosomes are present in a small space in mitotic cells (Fig. 4C), so it seems reasonable that the scattered individual and more extended chromosomes in immature oocytes do not exclude soluble molecules. We therefore subtracted nuclear from chromosomal fluorescence to get the value for bound Ran. As with the FRAP recovery, the relationship between bound Ran and added Ran appears to be characteristic of a single type of binding site (Fig. 6C). Fitting the curve yields a value of 30  $\mu\text{M}$  for the concentration of Ran-binding sites within the space occupied by the chromosomes.

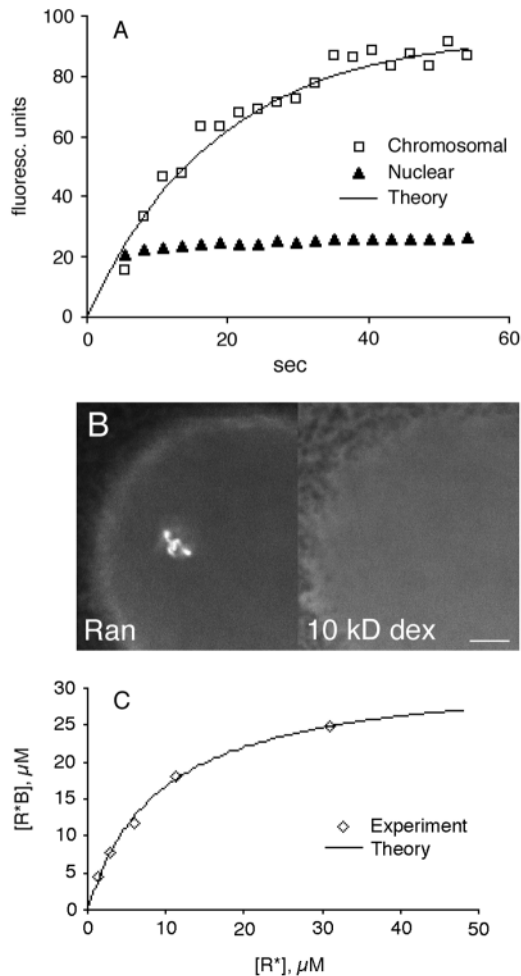


**Fig. 6.** Steady-state Ran association with chromosomes in immature starfish oocytes. (A) Recovery from photobleaching. Fluorescence from the brightest part of a chromosome was measured and is plotted by open squares whereas the nuclear fluorescence is denoted by filled triangles. The 0 second time point corresponds to the first post-bleach image where the nuclear and chromosomal fluorescence are set to 0 (symbols not shown at this time point because they would overlap). The fluorescence recovery at subsequent time points is equal to the increase in fluorescence relative to the fluorescence in the first post-bleach image. The nuclear fluorescence has already recovered by the second post-bleach image, and clearly recovers faster than the chromosomal fluorescence. If the chromosomal recovery is not limited by diffusion of soluble Ran, and if the interaction follows mass action kinetics with a single type of binding site, the chromosomal recovery should be exponential. The theory line shows an exponential recovery with rate constant  $0.06 \text{ second}^{-1}$ . (B) Oocytes were co-injected with Alexa 488 Ran ( $7 \mu\text{M}$  final concentration) and 10 kDa rhodamine dextran ( $100 \mu\text{g/ml}$ ) and were imaged separately with either the 488 nm line or the 568 nm line in the confocal microscope. The nucleus takes up most of the image, with the cytoplasm in the upper left corner of each image. The images show that the dextran is not excluded from the region of the chromosomes, probably because the chromosomes are not fully condensed in the meiosis-I-prophase-arrested oocytes. In other experiments, oocytes were injected with 10 kDa dextran alone, and z series sections failed to detect signs of volume exclusion. The lack of exclusion indicates that the nuclear fluorescence should be subtracted from the chromosomal fluorescence to get a more accurate value for the bound Ran. Bar,  $10 \mu\text{m}$ . (C) Binding curve for chromosomal Ran for different amounts of injected fluorescent Ran. The theory line shows the predicted values for the concentration of binding sites in the chromosomal space of  $30 \mu\text{M}$ ; the close correspondence supports the idea that the interaction is with a single type of binding site.

To determine the  $K_d$ , it is necessary to know the amount of free ligand that is available for binding. However, the endogenous Ran concentration in starfish oocytes is unknown. Furthermore, the fraction  $\alpha$  of the nuclear Ran that is available for binding to chromosomes is unknown. Much of nuclear Ran is probably bound to proteins such as import/export factors while a smaller amount exists as free Ran-GTP and Ran-GDP. It is not known which of these is the chromosome-binding unit. These uncertainties do not affect the above conclusions about binding to a single type of site, or the concentration of the sites, nor do they affect the FRAP determination of  $k_{\text{off}}$ . Also, even with these uncertainties, it is possible to estimate the sum  $(K_d/\alpha) + [R]$ , where  $[R]$  is the total endogenous nuclear Ran and  $\alpha$  is the fraction of the total nuclear Ran that is available for binding to chromosomes (see Materials and Methods). The data suggested that the sum of  $(K_d/\alpha) + [R]$  was 9–10  $\mu\text{M}$ . Estimates of nuclear Ran concentration in other cell types are in the range of 8–10  $\mu\text{M}$ . With these values,  $K_d < 1 \mu\text{M}$  and is smaller for smaller  $\alpha$ .

## Discussion

As the recent evidence for Ran involvement in M phase is based on work in *Xenopus* egg extracts, we investigated Ran's

distribution and dynamics in intact *Xenopus* eggs. Ran was localized by immunofluorescence to chromosomes of *Xenopus* meiosis-II-arrested eggs. Fluorescently tagged Ran localized to the chromosomes in the *Xenopus* eggs, as well as in starfish oocytes and embryos and mouse eggs. Anaphase was observed in artificially activated *Xenopus* eggs; to our knowledge, this is the first time that this has been imaged. In this system, it is necessary to image the spindle in the vertical orientation, so that the anaphase movements do not occur in one plane of focus. In starfish, the entire meiotic process and also the early mitotic divisions can be imaged with a more favorable orientation. In both *Xenopus* and starfish, Ran appeared to remain associated with the chromosomes to the same degree throughout M phase. In mammalian cultured cells, Ran was present throughout the spindle region. However, the condensed chromosomes exclude soluble molecules from the space they occupy. When this is taken into account, it is evident that Ran is associated with chromosomes in mammalian cultured cells, although to a lesser degree than in the other cells we observed.

An earlier report found no association of Ran with chromosomes in fixed or digitonin-permeabilized mitotic mammalian cells in culture (Ren et al., 1993). However, formaldehyde was used to fix the cells for immunofluorescence in that study, whereas we find that methanol fixation preserves

the chromosomal distribution. Also, there was no energy source in the digitonin-permeabilization medium. Stably associated molecules may remain bound under these conditions, but our data indicate a dynamic association of Ran with chromosomes, and it would not be expected that Ran would remain bound to the chromosomes under these conditions.

Our findings are more in agreement with recent *in vivo* and *in vitro* work. Ran was localized by immunofluorescence at kinetochores of chromosomes in *C. elegans* (Bamba et al., 2002). Transient association of Ran with condensed chromatin added to *Xenopus* extracts was seen (Zhang et al., 1999), and Ran binding to nucleoplasmin-decondensed sperm chromatin has been demonstrated (Bilbao-Cortes et al., 2002).

It is not known what constitutes the Ran chromosomal binding unit. Ran, in its GTP or GDP form, may bind by itself, or may bind to another protein(s), which then binds to chromosomes (see further discussion below). Even with these uncertainties, photobleaching and binding experiments indicate that the association of the Ran-binding unit follows mass action kinetics to a single type of binding site of relatively high concentration within the space occupied by the chromosomes (~30  $\mu\text{M}$ ) and that the  $k_{\text{off}}$  for binding is ~0.06  $\text{second}^{-1}$ . Because we are using a fluorescently tagged human Ran in starfish oocytes, the values for endogenous Ran may be different.

As for the chromosomal binding site for Ran, one possibility is that it is located on the protein RCC1. This protein is thought to be continuously associated with the chromosomes (Carazo-Salas et al., 1999), and since it is the only known GDP/GTP exchange factor for Ran, there must be a steady-state concentration of Ran bound to RCC1 owing to the turnover through RCC1. From *in vitro* studies of purified proteins, three kinetic steps are involved in the GDP/GTP exchange that occurs on RCC1; the slowest  $k_{\text{off}}$ , and therefore the likely rate-determining step, is ~20  $\text{second}^{-1}$  (Klebe et al., 1995b). This is much greater than the  $k_{\text{off}}$  value of 0.06  $\text{second}^{-1}$  measured for Ran association with starfish chromosomes. The discrepancy suggests that most of the chromosomal Ran is involved in an interaction with another protein and that the steady-state concentration of Ran bound to RCC1 is a small fraction of the chromosomal Ran. In support of this, a significant amount of Ran can still bind to sperm chromatin depleted of RCC1 (Bilbao-Cortes et al., 2002). Another possibility is that RCC1 is regulated during mitosis by modification or association with other proteins and that its kinetic properties measured *in vitro* are different from those *in vivo*.

Recent ideas regarding Ran's role in spindle assembly had predicted a Ran-GTP gradient at the chromosomes; this gradient was recently demonstrated (Kalab et al., 2002). However, there have been no predictions of a high concentration of Ran at the chromosomes. One possibility is that the chromosomal interactions that we observe keep Ran-GTP near the chromosomes. An analogy may be made with the sarcoplasmic reticulum in striated muscle. Calcium is stored in the sarcoplasmic reticulum lumen, but the calcium-binding protein calsequestrin is only located in the terminal cisternae, near the calcium release sites (Franzini-Armstrong and Protasi, 1997). In a similar way, Ran associations with chromosomes may serve to concentrate Ran-GTP in the area

of the cell where it will function. This is supported by the finding that the chromatin-bound Ran increases membrane vesicle association with chromatin in an *in vitro* assay for nuclear envelope reformation (Bilbao-Cortes et al., 2002).

We thank Linda Runft, Jason Kirk, Susan Krueger, Nathalie Daigle, Joel Beaudoin and Virginie Hachet for help with experiments, Evelyn Houliston for advice on immunofluorescence and Alicia Smith, Petr Kalab, Ann Cowan, Iain Mattaj and Ian Macara for useful discussions. We also thank Andrew Giusti, Laurinda Jaffe, Jim Galbraith and Tom Rapoport for advice and/or critical reading of the manuscript. Supported by grants to M.T. from the Patrick and Catherine Donaghy Foundation, the Human Frontier Science Program, and the NIH (RO1-GM60389). M.M.R. was a Howard Hughes Predoctoral Fellow in the Biological Sciences. B.S. was supported by National Institutes of Health grant 1P41RR13186-01A1 for the National Resource for Cell Analysis and Modeling.

## References

- Bamba, C., Bobiniec, Y., Fukuda, M. and Nishida, E. (2002). The GTPase Ran regulates chromosome positioning and nuclear envelope assembly *in vivo*. *Curr. Biol.* **12**, 503-507.
- Bilbao-Cortes, D., Hetzer, M., Langst, G., Becker, P. B. and Mattaj, I. W. (2002). Ran binds to chromatin by two distinct mechanisms. *Curr. Biol.* **12**, 1151-1156.
- Bischoff, F. R. and Ponstingl, H. (1991). Mitotic regulator protein RCC1 is complexed with a nuclear ras-related polypeptide. *Proc. Natl. Acad. Sci. USA* **88**, 10830-10834.
- Carazo-Salas, R. E., Guarguaglini, G., Gruss, O. J., Segref, A., Karsenti, E. and Mattaj, I. W. (1999). Generation of GTP-bound Ran by RCC1 is required for chromatin-induced mitotic spindle formation. *Nature* **400**, 178-181.
- Carazo-Salas, R. E., Gruss, O. J., Mattaj, I. W. and Karsenti, E. (2001). Ran-GTP coordinates regulation of microtubule nucleation and dynamics during mitotic-spindle assembly. *Nat. Cell Biol.* **3**, 228-234.
- Carroll, D. J., Albay, D. T., Terasaki, M., Jaffe, L. A. and Foltz, K. R. (1999). Identification of PLC gamma-dependent and -independent events during fertilization of sea urchin eggs. *Dev. Biol.* **206**, 232-247.
- Dasso, M. (2001). Running on Ran: nuclear transport and the mitotic spindle. *Cell* **104**, 321-324.
- Dasso, M., Seki, T., Azuma, Y., Ohba, T. and Nishimoto, T. (1994). A mutant form of the Ran/TC4 protein disrupts nuclear function in *Xenopus laevis* egg extracts by inhibiting the RCC1 protein, a regulator of chromosome condensation. *EMBO J.* **13**, 5732-5744.
- Desai, A. and Hyman, A. (1999). Microtubule cytoskeleton: No longer an also Ran. *Curr. Biol.* **9**, R704-R707.
- Desai, A., Maddox, P. S., Mitchison, T. J. and Salmon, E. D. (1998). Anaphase A chromosome movement and poleward spindle microtubule flux occur at similar rates in *Xenopus* extract spindles. *J. Cell Biol.* **141**, 703-713.
- Ellenberg, J., Siggia, E. D., Moreira, J. E., Smith, C. L., Presley, J. F., Worman, H. J. and Lippincott-Schwartz, J. (1997). Nuclear membrane dynamics and reassembly in living cells: targeting of an inner nuclear membrane protein in interphase and mitosis. *J. Cell Biol.* **138**, 1193-1206.
- Franzini-Armstrong, C. and Protasi, F. (1997). Ryanodine receptors of striated muscles: a complex channel capable of multiple interactions. *Physiol. Rev.* **77**, 699-729.
- Gallo, C. J., Hand, A. R., Jones, T. L. Z. and Jaffe, L. A. (1995). Stimulation of *Xenopus* oocyte maturation by inhibition of the G-protein  $\alpha_s$  subunit, a component of the plasma membrane and yolk platelet membranes. *J. Cell Biol.* **130**, 275-284.
- Gorlich, D. and Kutay, U. (1999). Transport between the cell nucleus and the cytoplasm. *Annu. Rev. Cell Dev. Biol.* **15**, 607-660.
- Gruss, O. J., Carazo-Salas, R. E., Schatz, C. A., Guarguaglini, G., Kast, J., Wilm, M., le Bot, N., Vernos, I., Karsenti, E. and Mattaj, I. W. (2001). Ran induces spindle assembly by reversing the inhibitory effect of Importin alpha on TPX2 activity. *Cell* **104**, 83-93.
- Heald, R. and Weis, K. (2000). Spindles get the ran around. *Trends Cell Biol.* **10**, 1-4.
- Hetzer, M., Bilbao-Cortes, D., Walther, T. C., Gruss, O. J. and Mattaj, I.

- W. (2000). GTP hydrolysis by Ran is required for nuclear envelope assembly. *Mol. Cell* **5**, 1013-1024.
- Jaffe, L. A., Gallo, C. J., Lee, R. H., Ho, Y. K. and Jones, T. L. (1993). Oocyte maturation in starfish is mediated by the beta gamma-subunit complex of a G-protein. *J. Cell Biol.* **121**, 775-783.
- Kahana, J. A. and Cleveland, D. W. (1999). Beyond nuclear transport. Ran-GTP as a determinant of spindle assembly. *J. Cell Biol.* **146**, 1205-1210.
- Kahana, J. A. and Cleveland, D. W. (2001). Cell cycle. Some importin news about spindle assembly. *Science* **291**, 1718-1719.
- Kalab, P., Pu, R. T. and Dasso, M. (1999). The ran GTPase regulates mitotic spindle assembly. *Curr. Biol.* **9**, 481-484.
- Kalab, P., Weis, K. and Heald, R. (2002). Visualization of a Ran-GTP gradient in interphase and mitotic *Xenopus* egg extracts. *Science* **295**, 2452-2456.
- Klebe, C., Bischoff, F. R., Ponstingl, H. and Wittinghofer, A. (1995a). Interaction of the nuclear GTP-binding protein Ran with its regulatory proteins RCC1 and RanGAP1. *Biochem.* **34**, 639-647.
- Klebe, C., Prinz, H., Wittinghofer, A. and Goody, R. S. (1995b). The kinetic mechanisms of Ran-nucleotide exchange catalyzed by RCC1. *Biochemistry* **34**, 12543-12552.
- Lemaitre, J.-M., Géraud, G. and Méchali, M. (1998). Dynamics of the genome during early *Xenopus laevis* development: karyomeres as independent units of replication. *J. Cell Biol.* **142**, 1159-1166.
- Macara, I. G., Brownawell, A. and Welch, K. (2000). Ran. In *GTPases* (ed. A. Hall), pp. 198-221. Oxford: Oxford University Press.
- Mattaj, I. W. and Englmeier, L. (1998). Nucleocytoplasmic transport: the soluble phase. *Annu. Rev. Biochem.* **67**, 265-306.
- Mehlmann, L. M. and Kline, D. (1994). Regulation of intracellular calcium in the mouse egg: Calcium release in response to sperm or inositol trisphosphate is enhanced after meiotic maturation. *Biol. Reprod.* **51**, 1088-1098.
- Moore, J. D. (2001). The Ran-GTPase and cell-cycle control. *Bioessays* **23**, 77-85.
- Murray, A. W. (1991). Cell cycle extracts. *Methods Cell Biology* **36**, 581-605.
- Nachury, M. V., Maresca, T. J., Salmon, W. C., Waterman-Storer, C. M., Heald, R. and Weis, K. (2001). Importin beta is a mitotic target of the small GTPase Ran in spindle assembly. *Cell* **104**, 95-106.
- Ohba, T., Nakamura, M., Nishitani, H. and Nishimoto, T. (1999). Self-organization of microtubule asters induced in *Xenopus* egg extracts by GTP-bound Ran. *Science* **284**, 1356-1358.
- Ohtsubo, M., Okazaki, H. and Nishimoto, T. (1989). The RCC1 protein, a regulator for the onset of chromosome condensation locates in the nucleus and binds to DNA. *J. Cell Biol.* **109**, 1389-1397.
- Ookata, K., Hisanaga, S., Okano, T., Tachibana, K. and Kishimoto, T. (1992). Relocation and distinct subcellular localization of p34cdc2-cyclin B complex at meiosis reinitiation in starfish oocytes. *EMBO J.* **11**, 1763-1772.
- Ren, M., Drivas, G., D'Eustachio, P. and Rush, M. G. (1993). Ran/TC4: a small nuclear GTP-binding protein that regulates DNA synthesis. *J. Cell Biol.* **120**, 313-323.
- Ribbeck, K., Lipowsky, G., Kent, H. M., Stewart, M. and Gorlich, D. (1998). NTF2 mediates nuclear import of Ran. *EMBO J.* **17**, 6587-6598.
- Rolls, M. M., Stein, P. A., Taylor, S. S., Ha, E., McKeon, F. and Rapoport, T. A. (1999). A visual screen of a GFP-fusion library identifies a new type of nuclear envelope membrane protein. *J. Cell Biol.* **146**, 29-44.
- Sazer, S. (1996). The search for the primary function of the Ran GTPase continues. *Trends Cell Biol.* **6**, 81-85.
- Sazer, S. and Dasso, M. (2000). The Ran decathlon: multiple roles of Ran. *J. Cell Sci.* **113**, 1111-1118.
- Shirai, H., Hosoya, N., Sawada, T., Nagahama, Y. and Mohri, H. (1990). Dynamics of mitotic apparatus formation and tubulin content during oocyte maturation in starfish. *Dev. Growth Diff.* **32**, 521-529.
- Terasaki, M., Runft, L. and Hand, A. (2001). Organization of the endoplasmic reticulum during *Xenopus* oocyte maturation and egg activation. *Mol. Biol. Cell* **12**, 1103-1116.
- Verlhac, M. H., Lefebvre, C., Guillaud, P., Rassini, P. and Maro, B. (2000). Asymmetric division in mouse oocytes: with or without Mos. *Curr. Biol.* **10**, 1303-1306.
- Wiese, C., Wilde, A., Moore, M. S., Adam, S. A., Merdes, A. and Zheng, Y. (2001). Role of importin- $\beta$  in coupling Ran to downstream targets in microtubule assembly. *Science* **291**, 653-656.
- Wilde, A. and Zheng, Y. (1999). Stimulation of microtubule aster formation and spindle assembly by the small GTPase Ran. *Science* **284**, 1359-1362.
- Wilde, A., Lizarraga, S. B., Zhang, L., Wiese, C., Glicksman, N. R., Walczak, C. E. and Zheng, Y. (2001). Ran stimulates spindle assembly by altering microtubule dynamics and the balance of motor activities. *Nat. Cell Biol.* **3**, 221-227.
- Zhang, C. and Clarke, P. R. (2000). Chromatin-independent nuclear envelope assembly induced by Ran GTPase in *Xenopus* egg extracts. *Science* **288**, 1429-1432.
- Zhang, C. and Clarke, P. R. (2001). Roles of Ran-GTP and Ran-GDP in precursor vesicle recruitment and fusion during nuclear envelope assembly in a human cell-free system. *Curr. Biol.* **11**, 208-212.
- Zhang, C., Hughes, M. and Clarke, P. R. (1999). Ran-GTP stabilises microtubule asters and inhibits nuclear assembly in *Xenopus* egg extracts. *J. Cell Sci.* **112**, 2453-2461.